

Supplemental Information

Conversion of Porous Anodic Al₂O₃ into Freestanding, Uniformly-aligned, Multi-wall TiO₂ Nanotube Arrays for Electrode Applications

John D. Berrigan,^{‡a} Taylor McLachlan,^{‡a} James R. Deneault,^b Ye Cai,^a Tae-Sik Kang,^b Michael F. Durstock^b and Kenneth H. Sandhage^{*a,c}

^aSchool of Materials Science and Engineering, and Air Force Center of Excellence on Bio-nano-enabled Inorganic/Organic Nanocomposites and Improved Cognition (BIONIC), Georgia Institute of Technology, 771 Ferst Drive, Atlanta, GA 30332-0245, U.S.A.

E-mail: ken.sandhage@mse.gatech.edu

^bMaterials and Manufacturing Directorate, Air Force Research Laboratory, Wright-Patterson Air Force Base, OH 45433-7702, USA

^cSchool of Chemistry and Biochemistry, Georgia Institute of Technology, 771 Ferst Drive Atlanta, GA, 30332, USA.

[‡]These authors contributed equally to this work.

Experimental Details

High-purity aluminum sheets (99.999% purity, 1 mm thick, Goodfellow Corp., Oakdale, PA, USA) were converted into porous anodic alumina (AAO) with aligned, one-end-closed pore channels on top of an Al backing following the anodization procedure reported by Kang, et al.¹ The templates were vacuum infiltrated with a titanium(IV) isopropoxide (97+% purity, Alfa Aesar, Ward Hill, MA, USA) solution (3:1 wt. ratio, in anhydrous isopropanol) and allowed to hydrolyze overnight in air (40% relative humidity). Excess TiO₂ formed during this process was removed using adhesive tape. The adhesive tape residue was removed by 30 min incubation in dichloromethane (99.9% purity, VWR, Radnor, PA, USA) under vigorous stirring. The infiltration process was then repeated a second time.

The TiO₂-infiltrated alumina was coated with a thin nitrocellulose-based film (Double Duty nail polish, Sally Hansen, Morris Plains, NJ) using a brush and allowed to dry for at least 2 h. This film masked the alumina and allowed for selective removal of the underlying Al backing by wet chemical etching in an aqueous solution of 0.25 M copper(II) chloride dihydrate (98% purity, Alfa Aesar, Ward Hill, MA, USA) in 6.0 M HCl (VWR, Radnor, PA, USA) at room temperature for ~20 min. The removal of Al also exposed the Al₂O₃ barrier layer that capped one end of the pore channels. This exposed Al₂O₃ barrier layer was dissolved by immersion in 3 M NaOH for 30 min at room temperature. This process both opened the AAO pores and widened the nanochannels. The nitrocellulose-based mask that had coated and protected the Al₂O₃ membrane was removed by dissolution in acetone. The pore-widened, TiO₂ infiltrated AAO template was then heated to 500°C for 1 h at a 5°C min⁻¹ ramp rate to crystallize the coating and pyrolyze residual organics. It is at this stage where single-wall titania nanotube (SWTNT) electrodes were transferred to FTO glass and integrated into DSSC electrodes following procedures described elsewhere.²

Coated AAO templates for multi-wall titania nanotube (MWTNT) conversion were then wrapped in nickel foil (25.4 μm thick, McMaster-Carr, Cleveland, OH, USA), and loaded into titanium tubes (2.5 cm diameter, 20 cm length; McMaster-Carr, Cleveland, OH, USA) containing a 3.6:1 molar ratio of TiF₄ (Advance Research Chemicals, Catoosa, OK, USA) to AAO and sealed in a glovebox under a high-purity Ar atmosphere. The ampoules were heated to 335°C for 8 h at a ramp rate of 5°C min⁻¹ to react Al₂O₃ and TiO₂ with TiF₄(g). After cooling, the as-reacted templates were exposed to a humid, flowing oxygen atmosphere at 250°C for 8 h to convert TiOF₂ into TiO₂, and then heated to 500°C for 1.5 h in air to further crystallize the reaction product. The procedure for etching, transferring the MWTNTs to FTO glass, and integration into DSSCs is described in detail elsewhere.²

The micro/nanoscale morphology of the AAO and MWTNTs were evaluated with scanning electron microscopy (1530 FEG SEM, LEO/Zeiss Electron Microscopy, Thornwood, NY) and transmission electron microscopy (JEOL 4000 EX, Japan Electron Optics Laboratory, Tachikawa, Tokyo). The crystal structures of the nanotube arrays were evaluated at room temperature via X-ray diffraction analyses (Alpha-1, PANalytical Corp., Almelo, The Netherlands). Current-voltage (I-V) measurements were conducted under AM 1.5G conditions (Oriel 300 Watt solar simulator, 100 mW cm⁻²) using an aperture with a measured area of 7.05 mm².

Supplemental Analyses

Dye desorption measurements were conducted to determine the amount of N719 dye (cis-di(thiocyanato-bis(2,2'-bipyridyl)-4,4'-dicarboxylato)) ruthenium(II) bis(tetrabutylammonium)) adsorbed onto SWTNT and MWTNT electrodes. After incubating in N719 dye for 24 h, then rinsing twice in dry acetonitrile, the dye was desorbed from the surfaces of the electrode by incubating in 2 mL of 0.1 M NaOH in water/ethanol, 1:1 vol. ratio for 5 min. The absorbance of the dye in solution was measured by UV-Vis spectroscopy and compared to six solutions of known N719 concentration (5 μM, 10 μM, 15 μM, 20 μM, 30 μM and 115 μM/159 μM). The instrument was calibrated using new solutions for each experiment. An example of typical UV-Vis spectra and the corresponding calibration curves using peak absorbance at 513 nm are shown in **Figure S1(a,b)** and **Figure S2(a,b)**. The fitted calibration curve was used to determine the concentration of N719 dye in the 0.1 M NaOH solutions using the peak absorbance of each electrode at 513 nm (Figure S3(c, d) and S4(c, d)). Given that 2 mL of solution was used to desorb the N719 dye, the number of moles of N719 desorbed from the MWTNT electrodes can be calculated. The dye loading

Supplemental Information

Chemical Communications

was then normalized to the area occupied on the FTO-bearing glass substrate by the SWTNT or MWTNT electrode. Optical image analyses (Image-J) were used to accurately measure such electrode area. More specifically, the optical micrographs taken of each electrode were passed through an image analysis macro that filtered the image based on whiteness using four grayscale thresholds. The area determined at each threshold was averaged to give the electrode area. This method compensated for the detrimental effect of void space in the electrode.

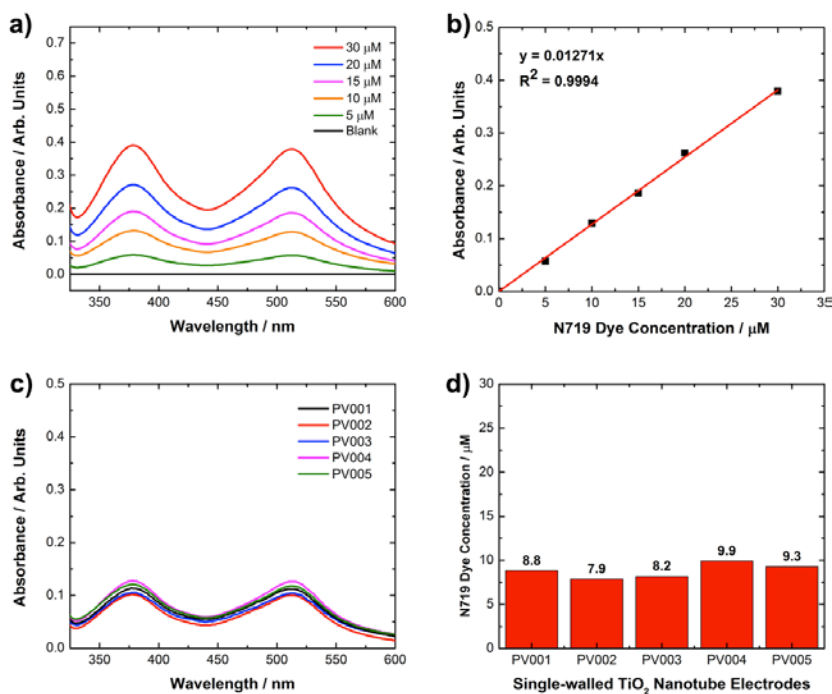


Figure S1. UV-Vis absorbance spectra of the N719 dye at various known concentrations (upper left). The absorbance at 513 nm was used to generate a calibration curve (upper right). UV-Vis absorbance spectra from 5 SWTNT electrodes (lower left), and the corresponding N719 dye concentration measured using the calibration curve (lower right).

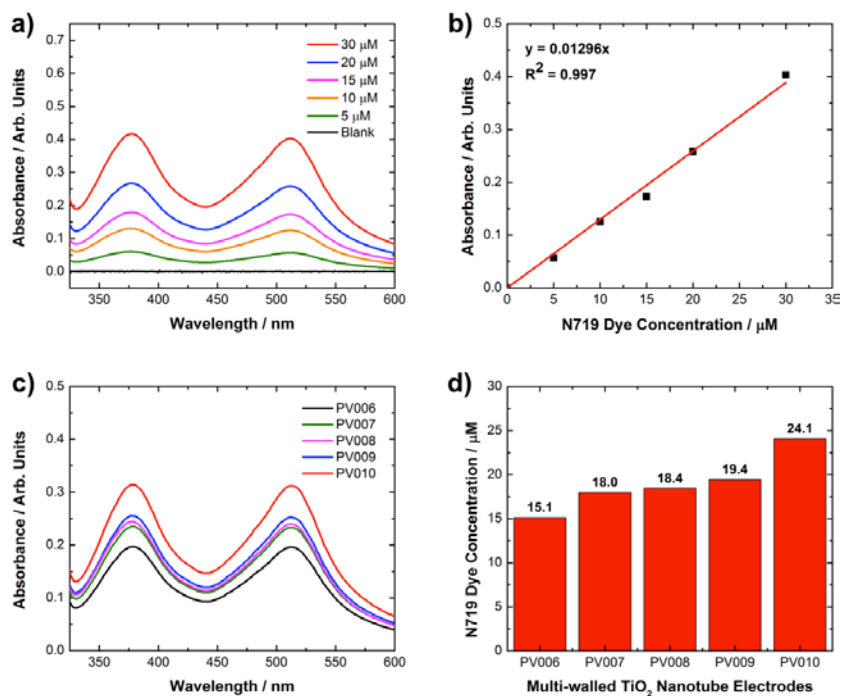


Figure S2. UV-Vis absorbance spectra of N719 at various known concentrations (upper left). The absorbance at 513 nm was used to generate a calibration curve (upper right). UV-Vis absorbance spectra from 5 MWTNT electrodes (lower left), and the corresponding N719 dye concentration measured using the calibration curve (lower right).

Supplemental Information

The current-voltage characteristics of five SWTNT- and MWTNT-bearing dye sensitized solar cells are shown in **Figures S3 and S4**, respectively, under dark and AM 1.5 simulated solar illumination conditions. These results indicated that the worst-performing MWTNT-based device exhibited a power conversion efficiency greater than that of the best-performing SWTNT-based device (4.7% vs. 4.0%).

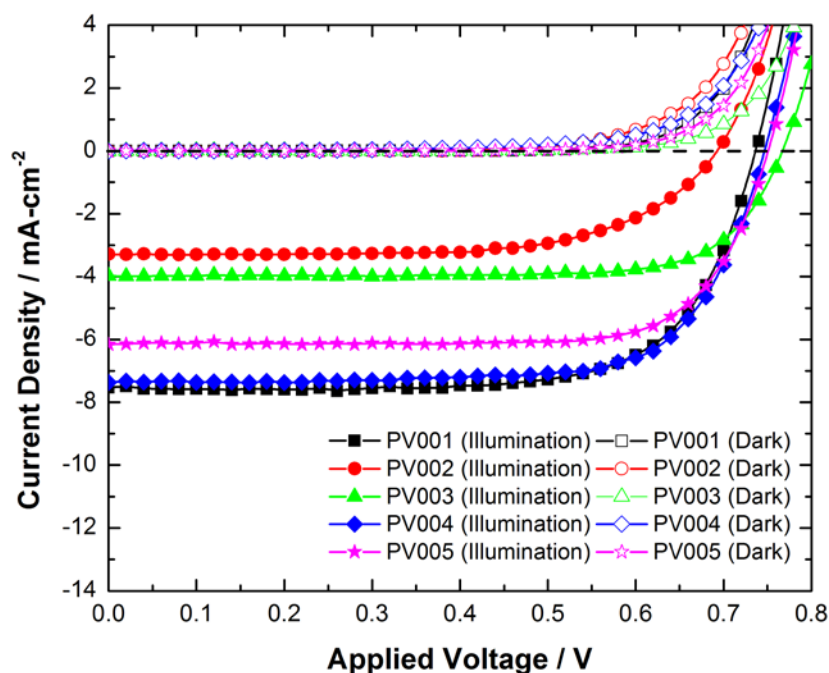


Figure S3. Current-voltage behavior of five dye-sensitized solar cells using SWTNT arrays as electrodes under both dark and illumination conditions.

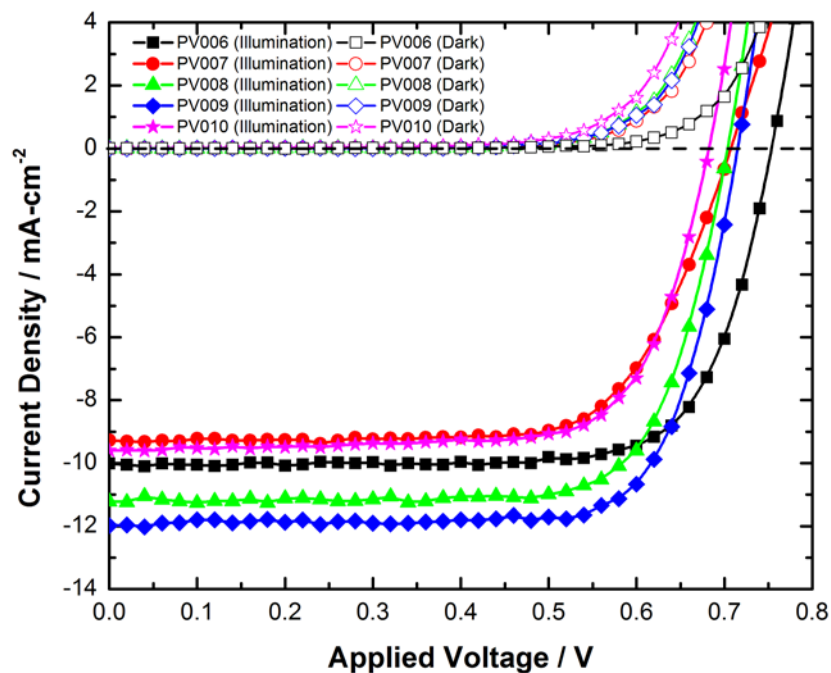


Figure S4. Current-voltage behavior of five dye-sensitized solar cells using MWTNT arrays as electrodes under both dark and illumination conditions.

Roughness Factor Calculations

The roughness factor or rugosity (f_r) of a surface is defined according to **Equation S.1**:³

$$f_r = \frac{A_r}{A_p} \quad (\text{S.1})$$

where A_r is the real (actual) surface area and A_p is the planar substrate (geometric) surface area. In DSSCs, the roughness factor is an estimate of the total internal surface area that is available for dye adsorption relative to its projected surface area. The real surface area can be measured (i.e., by Brunauer-Emmett-Teller surface area analysis) or estimated from measured dimensions. Roughness factor calculations for the synthesized aligned nanotube arrays synthesized were estimated based on geometric measurements obtained by electron microscopy. From measurements of the nanotube wall thickness, outer diameter, length, and channel center-to-channel center spacing, both A_r and A_p can be calculated.

Assuming that a given nanotube can be approximated as a smooth, symmetric, hollow cylinder with no porosity within the tube wall and negligible surface area at the top and bottom edges, the A_r is given by **Equation S.2**:

$$A_r = 2\pi l(r_1 + r_2) \quad (\text{S.2})$$

where l is the length of the cylinder and r_1 and r_2 are in the inner and outer radii of the nanotube.

The planar substrate area, A_p , is a two-dimensional area measurement of a three-dimensional object projected onto an arbitrary plane (in this case, the area per nanotube on the electrode surface). It was observed that, after dissolution of the anodic aluminum oxide (AAO) template, the nanotubes agglomerated in a near-hexagonal arrangement, as illustrated in **Figure S5**.

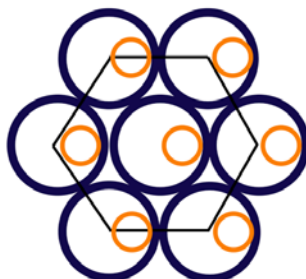


Figure S5: Schematic illustration of a multiwall titania nanotube array exhibiting hexagonal packing. The blue and orange circles represent the outer (reaction formed) and inner (coating derived) nanotubes, respectively.

This arrangement allowed for the estimation of the area density of nanotubes for each electrode (i.e., assuming a regular hexagon with side-length, t_{space} , equal to the channel center-to-channel center spacing). The area of a regular hexagon is given by **Equation S.3**.

$$A_{hexagon} = \frac{3\sqrt{3}}{2} t_{space}^2 \quad (\text{S.3})$$

For single-wall TiO₂ nanotubes (SWTNT) that pack into a periodic hexagonal array, three complete nanotubes lie within each hexagon (1 nanotube in the center and 6 nanotubes along the edges that contribute 1/3 each). For multi-wall TiO₂ nanotube (MWTNT) arrays, three complete pairs of nanotubes lie within the hexagon, as illustrate in Figure S5. The areal density of nanotubes in the array, $A_{density}$ (nanotubes per unit area), was determined by dividing the number of nanotubes within the hexagonal area, n_{tubes} , by the area of the hexagon (**Equation S.4**).

$$A_{density} = \frac{2n_{tubes}}{3t_{space}^2 \sqrt{3}} \quad (\text{S.4})$$

$$A_p = A_{density}^{-1} = \frac{3t_{space}^2 \sqrt{3}}{2n_{tubes}} \quad (\text{S.5})$$

The inverse of **Equation S.4** yields the planar surface area per nanotube within the array (**Equation S.5**). Combining **Equations S.2** and **S.5** with **Equation S.1** provides an estimate for the roughness factor of the electrodes used in this work.

Supplemental Information

Roughness Factor Calculation for Single-Wall TiO₂ Nanotube Arrays

Using the measured geometric parameters tabulated in **Table S.1**, a roughness factor was estimated for sol-gel-derived single-wall TiO₂ nanotube arrays using equations S.1, S.2, and S.5.

Table S.1. Measured parameters used to estimate the roughness factor for sol-gel derived SWTNT arrays.

Parameter	Symbol	Measured Value
Channel center-to-channel center spacing	t_{space}	398 ± 70 nm
Nanotube Length	l	13.2 ± 0.4 μm
Nanotube Wall Thickness	W_t	30 ± 10 nm
Nanotube Outer Radius	r_1	77 ± 20 nm

Subtracting the nanotube wall thickness (W_t) from the nanotube outer radius (r_1) yielded the value for the inner nanotube radius, r_2 . These values were inserted into equation S.2. The calculation of A_r is shown, in full, from equations S.6 to S.8. The estimated value of A_r was $10 \mu\text{m}^2$.

$$A_r = 2\pi \cdot (13.2 \mu\text{m}) \cdot (0.077 \mu\text{m} + 0.043 \mu\text{m}) \quad (\text{S.6})$$

$$A_r = 2\pi \cdot (13.2 \mu\text{m}) \cdot (0.12 \mu\text{m}) \quad (\text{S.7})$$

$$A_r = 10.0 \mu\text{m}^2 \quad (\text{S.8})$$

To calculate the planar area (A_p) the channel center-to-channel center distance was entered into equation S.5 where $n_{tubes} = 3$. The results of the calculation are shown in equations S.10 to S.13 and yielded an estimated roughness factor of 75 for SWTNT arrays.

$$A_p = A_{density}^{-1} = \frac{3(0.398 \mu\text{m})^2 \sqrt{3}}{2 \cdot 3} \quad (\text{S.9})$$

$$A_p = \frac{0.823 \mu\text{m}^2}{6} \quad (\text{S.10})$$

$$A_p = 0.137 \mu\text{m}^2 \quad (\text{S.11})$$

$$f_r = \frac{10.0 \mu\text{m}^2}{0.137 \mu\text{m}^2} = 73.0 \quad (\text{S.12})$$

Roughness Factor Calculation for Multi-Wall TiO₂ Nanotube Arrays

Using the measured geometric parameters tabulated in **Table S.2**, a roughness factor was estimated for sol-gel-derived single-wall TiO₂ nanotube arrays using equations S.1, S.2, and S.5.

Table S.2 Measured parameters used to estimate the roughness factor for MWTNT arrays.

Parameter	Symbol	Measured Value
Channel center-to-channel center spacing	t_{space}	398 ± 70 nm
Nanotube Length	l	13.2 ± 0.4 μm
Nanotube Wall Thickness	W_t	80 ± 13 nm
Nanotube Outer Radius	r_1	213 ± 38 nm

Subtracting the nanotube wall thickness (W_t) from the nanotube outer radius (r_1) yielded the value for the inner nanotube radius, r_2 . These values were input into equation S.2. The calculation of A_r is shown, in full, from equations S.13 to S.16. The estimated value of A_r was $38.7 \mu\text{m}^2$.

$$A_r = 2\pi \cdot (13.2 \mu\text{m}) \cdot (0.077 \mu\text{m} + 0.043 \mu\text{m}) \\ + 2\pi \cdot (13.2 \mu\text{m}) \cdot (0.213 \mu\text{m} + 0.133 \mu\text{m}) \quad (\text{S.13})$$

$$A_r = 2\pi \cdot (13.2 \mu\text{m}) \cdot (0.12 \mu\text{m}) \\ + 2\pi \cdot (13.2 \mu\text{m}) \cdot (0.346 \mu\text{m}) \quad (\text{S.14})$$

$$A_r = 9.95 \mu\text{m}^2 + 28.7 \mu\text{m}^2 \quad (\text{S.15})$$

$$A_r = 38.7 \mu\text{m}^2 \quad (\text{S.16})$$

To calculate the planar area (A_p) the channel center-to-channel center distance was entered into equation S.5 where $n_{tubes} = 3$. The results of the calculation are shown in equations S.17 to S.20 and yielded an estimated roughness factor of 282 for aligned MWTNT arrays.

$$A_p = A_{\text{density}}^{-1} = \frac{3(0.398 \mu\text{m})^2 \sqrt{3}}{2 \cdot 3} \quad (\text{S.17})$$

$$A_p = \frac{0.823 \mu\text{m}^2}{6} \quad (\text{S.18})$$

$$A_p = 0.137 \mu\text{m}^2 \quad (\text{S.19})$$

$$f_r = \frac{38.7 \mu\text{m}^2}{0.137 \mu\text{m}^2} = 282 \quad (\text{S.20})$$

References

1. T.-S. Kang, A. P. Smith, B. E. Taylor and M. F. Durstock, *Nano Lett.*, 2009, **9**, 601-606.
2. J. D. Berrigan, T.-S. Kang, Y. Cai, J. R. Deneault, M. F. Durstock and K. H. Sandhage, *Adv. Funct. Mat.*, 2011, **21**, 1693-1700.
3. R. N. Wenzel, *The Journal of Physical and Colloid Chemistry*, 1948, **53**, 1466-1467.